Increased amplifier spacing in a soliton system with quantum-well saturable absorbers and spectral filtering

D. Atkinson

Optoelectronics Research Centre, Department of Electronic and Electrical Engineering, University College London, Torrington Place, London WC1E 7JE, UK

W. H. Loh, V. V. Afanasjev, and A. B. Grudinin

Optoelectronics Research Centre, University of Southampton, Southampton SO9 5NH, UK

A. J. Seeds

Optoelectronics Research Centre, Department of Electronic and Electrical Engineering, University College London, Torrington Place, London WC1E 7JE, UK

D. N. Payne

Optoelectronics Research Centre, University of Southampton, Southampton S09 5NH, UK

Received April 11, 1994

The spacing between optical amplifiers in a long-haul soliton system may be increased to 100 km by using only passive quantum-well saturable absorbers and narrow-band filters for soliton control. After transmission over 9000 km at 10 Gbits/s, the effects of soliton–soliton interaction and Gordon–Haus jitter in the proposed system yield bit error rates of better than 10^{-9}.

Optically amplified soliton systems are an attractive solution to the problems imposed by fiber dispersion for high-bit-rate, long-distance telecommunications. However, Gordon–Haus timing jitter[1] and soliton–soliton interactions[2] degrade system performance. Narrow-band filters help to control solitons, but the additional amplification required leads to the growth of low-level nonsoliton radiation that interacts detrimentally with the solitons. Filters have shown enhanced performance when used with synchronous modulation for active soliton control[3] or when used as sliding filters.[4] Alternatively, the introduction of nonlinear gain, or saturable absorption (SA), can preferentially suppress the nonsoliton radiation[5,6] and in the case of SA give unlimited stable soliton propagation.[7].

In this Letter we demonstrate theoretically the use of multiple-quantum-well (MQW) saturable absorbers with narrow-band filters in a 9000-km, 10-Gbit/s system. The amplifier spacing may be increased from the 50 km typical of the schemes mentioned above to 100 km, a separation shown possible only with active control.[8] At normal incidence, InP-based MQW material offers a passive, compact, polarization-insensitive, fast saturable absorber on a low-loss substrate. The component arrangement modeled is MQW, filter, fiber, and amplifier, as depicted in Fig. 1; this is repeated along the 9000-km span.

In the SA model,[9] photogenerated excitons decay with a fast time constant τ_f to free carriers, which in turn recombine with a slower time constant τ_s. Both free carriers and excitons (with normalized densities x and y, respectively) screen absorption. The screening is calculated with a Runge–Kutta method to solve these equations[9]:

$$\frac{\mathrm{d}x}{\mathrm{d}t} = \frac{2\overline{\alpha}I}{\tau_s I_s} - \frac{x}{\tau_f}, \qquad \frac{\mathrm{d}y}{\mathrm{d}t} = \frac{1}{2}\frac{x}{\tau_f} - \frac{y}{\tau_s}, \tag{1}$$

where $\overline{\alpha} = 1 - x - y$; under cw illumination, $\overline{\alpha} = 1/2$ when I is equal to the saturation intensity I_s. With the small-signal absorption coefficient α_0, the saturable absorption coefficient is given by $\alpha(I, t) = \overline{\alpha}\alpha_0$.

Typical MQW parameters[10] are $\alpha_0 \approx 10^4\ \mathrm{cm}^{-1}$, $\tau_f \approx 300$ fs, $\tau_s \approx 1$ ns, and $I_s \approx 2\ \mathrm{kW/cm}^2$, though I_s can be varied considerably through barrier design. To discriminate low-level radiation from solitons we require I_s to be comparable to the soliton peak intensity ($\approx 130\ \mathrm{kW/cm}^2$ for 38 mW of peak power focused into 30 $\mu\mathrm{m}^2$). We also require near-complete recovery of the unsaturated absorption in a time scale shorter than the 100-ps interpulse spacing for 10-Gbit/s operation. Picosecond lifetimes can be obtained from low-temperature molecular-beam-epitaxy-grown material,[11] or carriers can be swept out with a dc reverse electrical bias. Reduction of the free carrier lifetimes will result in a corresponding increase in saturation intensity, and we use $\tau_s = 10$ ps and $I_s = 200\ \mathrm{kW/cm}^2$. Using biased devices with different barrier structures, Wood *et al.*[12] observed values of I_s both greater

0146-9592/94/191514-03$6.00/0

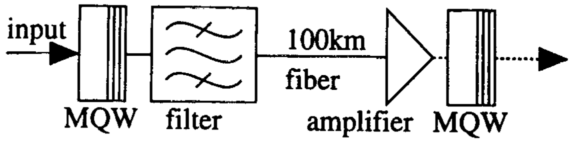

Fig. 1. Schematic showing the order of components.

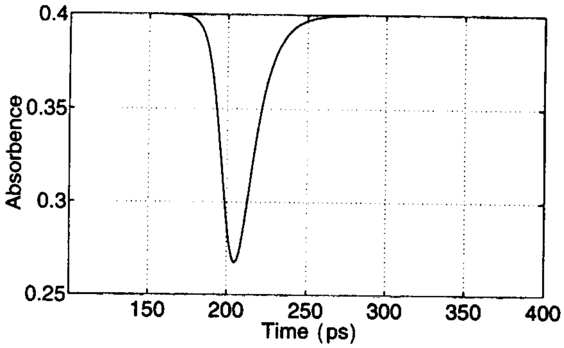

Fig. 2. Absorbance $\alpha(I, t)d$ as a pulse centered at 200 ps passes through the MQW.

and less than 200 kW/cm^2. Figure 2 plots the calculated response of the saturable absorber to the initial pulse with a FWHM T_{FWHM} of 15 ps and a peak intensity of 127 kW/cm^2. The other parameters are $\tau_f = 300$ fs and $\alpha_0 d = 0.4$, where d is the total quantum-well thickness and corresponds to 50–100 wells, depending on α_0.

Intensity- and time-dependent absorption changes $\Delta\alpha(I, t)$ lead to refractive-index changes $\Delta n(I, t)$ and a subsequent chirping of the soliton. We use the relationship $\Delta n(I, t) = C\Delta\alpha(I, t)$, where C is taken as 2.4×10^{-7} m (corresponding to a linewidth-enhancement factor[13] of 2) and $\Delta\alpha(I, t) = \alpha(I, t) - \alpha_0$. In reality C is wavelength and intensity dependent; however, to simplify our model we keep C constant but choose a value from the index changes observed by Ehrlich *et al.*[14] ($\Delta n = -0.12$, $\Delta\alpha = -5000\ cm^{-1}$).

The filter has amplitude transmission function $H(f) = (1 + 2if/B)^{-1}$, where f is the frequency relative to the initial pulse center frequency, and we choose $B = 60$ GHz. Propagation in the fiber was modeled using the split-step Fourier method with the following parameters: dispersion $D = 0.45$ ps/(nmkm), loss 0.23 dB/km, nonlinear index coefficient $n_2 = 2.7 \times 10^{-20}\ m^2\ W^{-1}$, effective core area $A_{eff} = 50\ \mu m^2$, operating wavelength λ of 1557 nm, and a constant linear time shift of 0.0366 ps/km. Pulses are launched with the form $P_0\ \mathrm{sech}^2(\tau/\tau_0)$, where $\tau_0 = T_{FWHM}/1.76$, $T_{FWHM} = 15$ ps, and $P_0 = 38$ mW. We assume saturated amplifiers, which maintain the average energy of a pulse stream constant. We first determine the gains G of each amplifier with distance z along the line such that the soliton energy remains constant and keep these values of $G(z)$ fixed for subsequent calculations (with amplifier noise, soliton-soliton interaction or different values of P_0). For different MQW or filter parameters, $G(z)$ is recalculated. In the absence of the saturable absorber, Fig. 3 shows that the solitons are unstable and break up (note that the dispersion length is 125 km). With the saturable absorber, Fig. 4 demonstrates that soliton propagation is stable for at least 9000 km. Along the whole transmission line, $G(z)$ varies by only 0.1 dB (additional calculations with G constant showed stable propagation, although the initial oscillations of the pulse peak intensity were more pronounced).

The stability is also insensitive to the chirp imparted by the absorber. We have observed stable propagation with the sign of C reversed and with $C = 0$. The pulse is not a true soliton in the lossy fiber, and this generates chirp that is generally larger than the absorber-induced chirp. At 5000 km, the FWHM of the pulses after each amplifier is 15.6 ps; when $C = 0$, this FWHM is 14.4 ps, indicating that in this filtered system the SA's contribution to the pulse chirp is relatively minor. Following amplification, the SA action decreases the pulse width from 15.6 to 15.3 ps, the filter reduces pulse chirp and increases its temporal width to 17.2 ps, and the pulse then narrows over the first 70 km of fiber before broadening to 15.6 ps.

Figure 5 shows the propagation of two solitons, initially in phase with separation 100 ps (a bit rate of 10 Gbits/s). After 9000 km, soliton–soliton interactions lead to a pulse peak separation of 101 ps. The mean power after each amplifier, assuming an equal proportion of 1's and 0's, is 5 dBm. For calculation of the Gordon–Haus timing jitter, each amplifier introduces on the pulse a random frequency shift with variance $\langle\overline{\Omega}^2\rangle$ given by[15]

$$\langle\overline{\Omega}^2\rangle = \frac{(2\pi c)^2 h n_2 N_{sp}(G - 1)}{3\tau_0 D \lambda^4 A_{eff} Q}, \qquad (2)$$

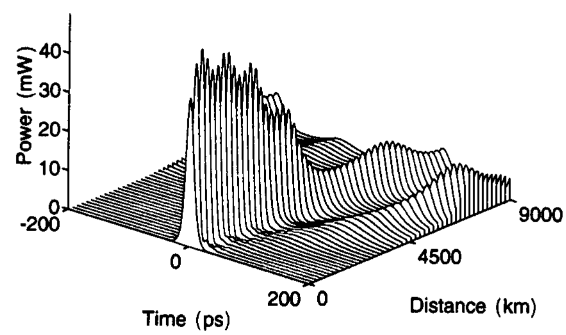

Fig. 3. Pulse at launch and after every second amplifier with filters but no saturable absorbers.

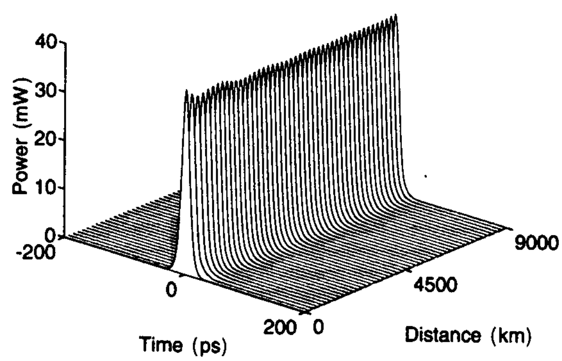

Fig. 4. Same as Fig. 3 but with saturable absorbers.

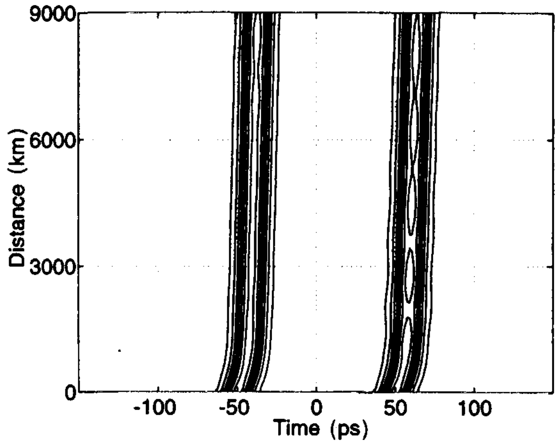

Fig. 5. Contour plot showing little interaction between two solitons.

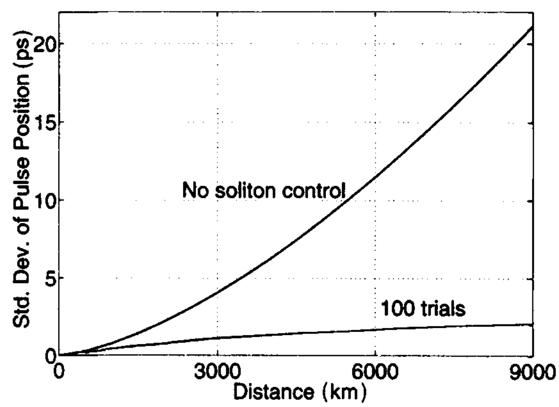

Fig. 6. Standard deviations of pulse positions showing the Gordon–Haus limit and the jitter after 100 trials.

where N_{sp} is taken to be 1.0, G is the amplifier gain, and Q is P_0/P_f, P_f being the peak power of the fundamental soliton (3.7 mW here). Figure 6 plots the standard deviation of pulse positions with no filtering or SA[15] and the result of 100 trials of our model. We determined the pulse positions T by using $T = \int |\psi|^2 t \mathrm{d}t / \int |\psi|^2 \mathrm{d}t$, where ψ is the pulse amplitude. After 9000 km, the standard deviation of the jitter is only 2.1 ps. For a bit error rate of 10^{-9} the pulse jitter should be less than 33 ps/6.1 = 5.5 ps for 10-Gbit/s operation.[1] In this model, amplifier noise shifts the pulse frequency, but there is no explicit addition of intensity noise (though random frequency shifts lead to differing filter losses). To demonstrate stability against intensity fluctuations, the launch power P_0 was varied by $\pm 10\%$, and stable propagation was still achieved with oscillations in pulse energy of less than $\pm 5\%$ after the first 2000 km.

Finally the results are not very sensitive to various system parameters. For example, the filter was replaced with a filter having a $\cos^2$ power transmission, with free spectral range 120 GHz; separately the lifetime τ_s was reduced to 1 ps, and in a third simulation the saturation intensity I_s was reduced to 20 kW/cm^2. In each case we obtained stable propagation. The soliton–soliton interactions lead to a pulse separation different from 100 ps by less than 1.5 ps and a timing jitter standard deviation less than 2.5 ps.

Unlike sliding filters, the absorption spectra of MQW's limit their use in wavelength-division-multiplexed systems. Although a time-domain filtering process, saturable absorption can in principle be wavelength specific and thus wavelength-division-multiplexed compatible (for example, quantum dot materials have delta-function-like absorption spectra).

In summary, MQW material offers a compact, polarization-insensitive, passive saturable absorber. We have theoretically demonstrated their use in combination with narrow-band filtering in a soliton system to increase the amplifier spacing to 100 km. For a long-haul system of 9000 km operating at 10 Gbits/s with mean power of only 5 dBm, the effects of soliton–soliton interactions and Gordon–Haus jitter yield bit error rates of better than 10^{-9}.

References

1. J. P. Gordon and H. A. Haus, Opt. Lett. **11,** 665 (1986).
2. F. M. Mitschke and L. F. Mollenauer, Opt. Lett. **12,** 355 (1987).
3. M. Nakazawa, K. Suzuki, E. Yamada, H. Kubota, Y. Kimura, and M. Takaya, Electron. Lett. **29,** 729 (1993).
4. L. F. Mollenauer, E. Lichtman, M. J. Neubelt, and G. T. Harvey, Electron. Lett. **29,** 910 (1993).
5. Y. Kodama, M. Romagnoli, and S. Wabnitz, Electron. Lett. **28,** 1981 (1992).
6. M. Matsumoto, H. Ikeda, and A. Hasegawa, Opt. Lett. **19,** 183 (1994).
7. V. V. Afanasjev, W. H. Loh, A. B. Grudinin, D. Atkinson, and D. N. Payne, in *Conference on Lasers and Electro-Optics,* Vol. 8 of 1994 OSA Technical Digest Series (Optical Society of America, Washington, D.C., 1994), paper CThN1.
8. H. Kubota and N. Nakazawa, Electron. Lett. **29,** 1780 (1993).
9. H. A Haus and Y. Silberberg, J. Opt. Soc. Am. B **2,** 1237 (1985).
10. J. S. Weiner, D. B. Pearson, D. A. B. Miller, D. S. Chemla, D. Sivco, and A. Y. Cho, Appl. Phys. Lett. **49,** 531 (1986).
11. S. Gupta, J. F. Whitaker, and G. A. Mourou, IEEE J. Quantum Electron. **28,** 2464 (1992).
12. T. H. Wood, T. Y. Chang, J. Z. Pastalan, C. A. Burrus Jr., N. J. Sauer, and D. C. Johnson, Electron. Lett. **27,** 257 (1991).
13. C. H. Henry, IEEE J. Quantum Electron. **QE-18,** 259 (1982).
14. J. E. Ehrlich, D. T. Neilson, A. C. Walker, and M. Hopkinson, Opt. Commun. **102,** 473 (1993).
15. D. Marcuse, J. Lightwave Technol. **10,** 273 (1992).